

## **EXPERIMENTAL INVESTIGATION OF SIZE EFFECT IN CONCRETE UNDER UNIAXIAL TENSION**

Marcel R.A. van Vliet and Jan G.M. van Mier  
Faculty of Civil Engineering and Geo Sciences  
Delft University of Technology  
Delft, The Netherlands

### **Abstract**

A research program was started to investigate size effect on strength and fracture energy of concrete under uniaxial tension. In a uniaxial tension test the stress gradients within the specimen are small compared to other frequently used tests like three-point-bend or eccentric compression tests. For this reason the size effect that is found can be attributed to the material rather than the type of test. Uniaxial tension tests have been carried out on dog-bone shaped specimens of six sizes in a range of 1:32. The tests were carried out with rotating boundary conditions. Using the maximum deformation measured at the specimen surface as feed-back signal stable test results have been obtained for all specimen sizes. Values for the nominal strength and fracture energy are derived and their sensitivity is studied. Based on these results the extrapolation towards small and large sizes is discussed as well as a possible explanation for the size effect on strength.

Key words: Size effect, uniaxial tension, nominal strength, fracture energy

### **1 Introduction**

The fact that concrete exhibits size effects has been known for long. Already in 1972 Walsh reported a size dependence of the nominal tensile stress that was found in three-point-bend tests on plain concrete beams, Walsh (1972).

Later on, his findings were confirmed by many other experimental investigations incorporating different kinds of tests. The experiments that have been conducted until now show furthermore a dependence of the size effect on the type of test. In general, one could say that the strength decrease with increasing specimen size is stronger when larger stress gradients are present within the specimen.

During the last decades an increasing experimental knowledge as well as new testing techniques allowed for the investigation of the softening behaviour of concrete. Measures for the post-peak resistance of concrete were introduced by Hillerborg and co-workers (Hillerborg et al. (1976)) and experimental as well as numerical investigations indicate that also for the fracture energy concrete exhibits size effect.

The research on size effect has brought an increasing insight in the effects underlying this phenomenon. Simultaneously, well known models like the Size Effect Law by Bažant (1984) or the Multi Fractal Scaling Law by Carpinteri et al. (1994) attempt to extrapolate the available experimental results to smaller and larger specimen sizes. A study by Mulmule et al. (1995), using results of ice tests in a scale range of 1:160, showed however that the predictions of the previously mentioned models strongly depended on the size range on which the fit was based. This leads to the conclusion that a true understanding of the size effect phenomenon can only be achieved by getting more insight in the physical mechanisms underlying the size effect. Models incorporating these physical mechanisms can then be used to go beyond the laboratory size range and predict the behaviour of full size structures.

The aim of the research presented in this paper is to study size effect on strength and fracture energy of concrete under uniaxial tension. Apart from tests carried out by Bažant and Pfeiffer (1987) and Ferro (1994) few experimental results are available on this topic. The aforementioned experiments comprised tests in a size range of 1:4 under rotating, and 1:16 under controlled boundary conditions respectively. In the current research program uniaxial tension tests are carried out on specimens of six different sizes in a scale range of 1:32. During the tests the specimen ends are allowed to rotate freely in both the in-plane and the out-of-plane direction, thus ensuring a minimum influence of the boundary conditions.

The paper first describes the starting points of the test program, followed by an outline of the experimental techniques that have been used to perform the uniaxial tension tests: Results are presented of a series of tests on concrete specimens. In the discussion emphasis is placed on the sensitivity of the experimental values for corrections, and a possible explanation is offered for the observed size dependence of the nominal strength.

## 2 Experimental program

### 2.1 Specimens and concrete properties

The choice of the specimen shape, testing range and concrete mix properties were all closely related. Although prismatic specimens scaled in three dimensions are preferred in an investigation like this, practical considerations often have to prevail. Without the presence of a preferential area for crack initiation for instance, a huge area would have to be controlled for the largest specimens whereas also the risk of glue failure would be considerable. By using notched specimens part of these problems are solved but simultaneously large stress concentrations are introduced, Van Vliet and Van Mier (1998). The effects of these stress concentrations on the fracture process in relation to varying specimen size are still unclear. A middle course between preferences and practical feasibility therefore led to a range of six dog-bone shaped specimens with a constant thickness of 100 mm (denoted A to F in Fig. 1).

The width and height of each subsequent specimen size is scaled by a factor two. The specimens are cast using a concrete mix with a maximum grain size  $d_{max}=8$  mm and an average cube compressive strength of 50 MPa after 28 days (Table 1). For the smallest specimen the characteristic specimen size  $D$  was fixed at 50 mm, resulting in a smallest cross section of  $0.6D = 30$  mm. This is just inside the range of 3 to 5 times  $d_{max}$  which is usually taken as lower bound for the smallest representative volume.

All specimens were cast horizontally and compacted using vibration needles of 2 different sizes, which is described in detail in Van Vliet and Van Mier (1997). After two days the specimens were demoulded and placed under laboratory conditions. At an age between 56 and 61 days the specimens were tested. In order to account for the fact that only five specimens could be tested per week the specimens were cast in ten batches, with an even distribution of the specimen sizes over the various batches. To check

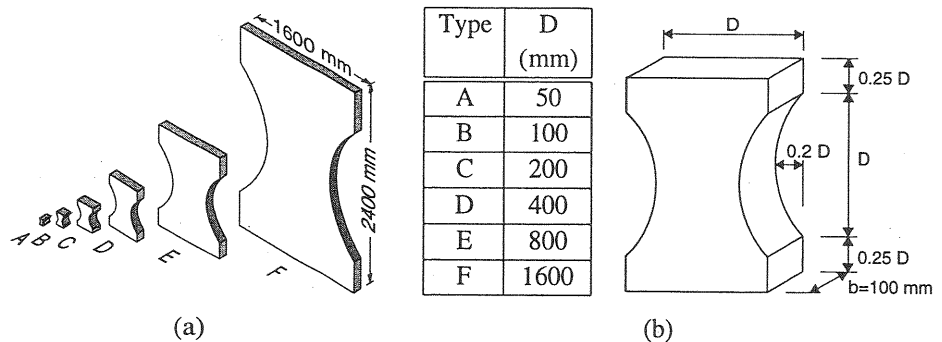


Fig. 1. Full specimen range of 1:32 (a) and specimen proportions (b)

Table 1. Concrete mix properties

Unit content kg/m <sup>3</sup>							w/c
8-4*	4-2*	2-1*	1-0.5*	0.5-0.25*	0.25-0.125*	PCB	
540	363	272	272	234	127	375	0.5

\* grain size in mm, PCB = Portland Cement B

for variations in batch strengths, 12 control cubes were cast from each batch and stored under water at a constant temperature of 20°C. After 28 days the cubes were tested in standard cube compression tests and tensile splitting tests.

## 2.2 Experimental set-ups and control system

The uniaxial tension tests have been conducted with rotating boundary conditions. For this purpose hinge constructions of three different sizes were designed, allowing for free rotations in both the in-plane and the out-of-plane direction, Van Vliet and Van Mier (1998). Within each hinge specimens of two subsequent sizes were tested. In order to avoid the need for continuous (major) adjustments of the set-ups, the hinges were placed in separate loading frames. Before testing, steel loading platens were glued to the specimens with a two-component epoxy resin after which specimen and loading platens were bolted to the hinge constructions.

Test control was obtained using a system that shows resemblance with the one applied by Li et al. (1993). Starting point is that the control LVDTs on all specimen sizes have a constant measuring length of 75 mm. In this way snap-back behaviour is avoided because the critical measuring length will not be exceeded. Large specimen areas were controlled by placing a number of control LVDTs in line along the edge of the specimen, both on the front and the back side. A newly developed control device continuously checks up to 16 LVDTs for the one measuring the largest deformation. This LVDT is used to control the test. When the next instant another LVDT measures a larger deformation test control is switched to that LVDT. Because of the limited number of LVDTs that can be handled by the control device it was not possible to control all four edges of the biggest specimen. For this reason a small load eccentricity was applied for all specimens to ensure crack initiation at the side of the specimen where the control LVDTs were placed. The eccentricity, which is obtained by glueing the loading platens slightly eccentrically, is scaled with the specimen size (1 mm for the A, to 32 mm for the F specimens). Thus, according to the theory of linear elasticity, the stress in the outermost fibre is equal for all specimen sizes. In all tests a constant deformation rate of 0.028  $\mu\text{m/s}$  was applied.

### 2.3 Measurements

The aim of the current experimental investigation is to get more insight in the physical mechanisms causing size effect of concrete. For this reason various surface measurements were made during each test. Examples of the measurements taken on a B and D specimen are shown in Fig. 2. Along the edges of a specimen a number of control LVDTs is placed in line, each with a measuring length of 75 mm ( $L_c$ ). In the middle of all specimens measurements with a scaled measuring length  $L_s$  were taken, varying from 30 mm for the A specimens up to 960 mm for the F specimens. These measurements proved to be very useful for mutual comparisons between the different specimen sizes, because they span the same part of each specimen. Besides the scaled deformations and the deformations used for test control, deformations were measured spread over the specimen surface to monitor the crack propagation.

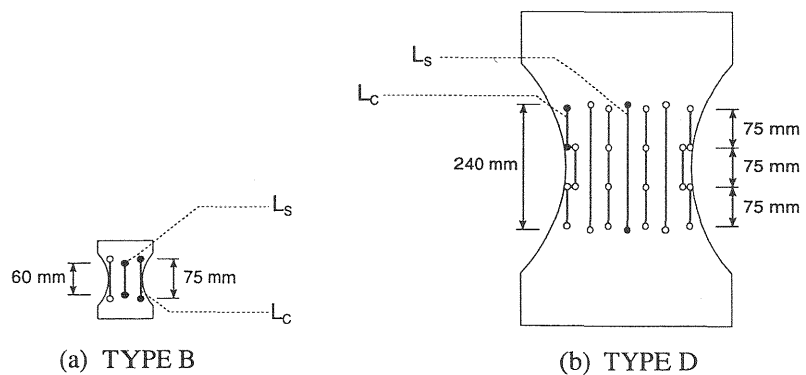


Fig. 2. Placing of displacement transducers on specimen B (a) and D (b)

## 3 Results

### 3.1 Softening curves and nominal strength

At least four successful tests were conducted for each specimen size. The resulting force-deformation curves are shown in Figs. 3a and b, where the deformation is the average deformation of the scaled measurements  $L_s$  on the front and the back side of a specimen (Fig. 2). The measured forces have been corrected for the dead weight of the upper loading platen and the part of the specimen above the crack. The weight of the specimen part below the crack, the lower loading platen and the lower hinge construction are incorporated in the measured force and can be seen as a constant, uncontrollable part of the external load. The tests were continued until the first control LVDT went out of range, which was at 500  $\mu\text{m}$ . Because of the large

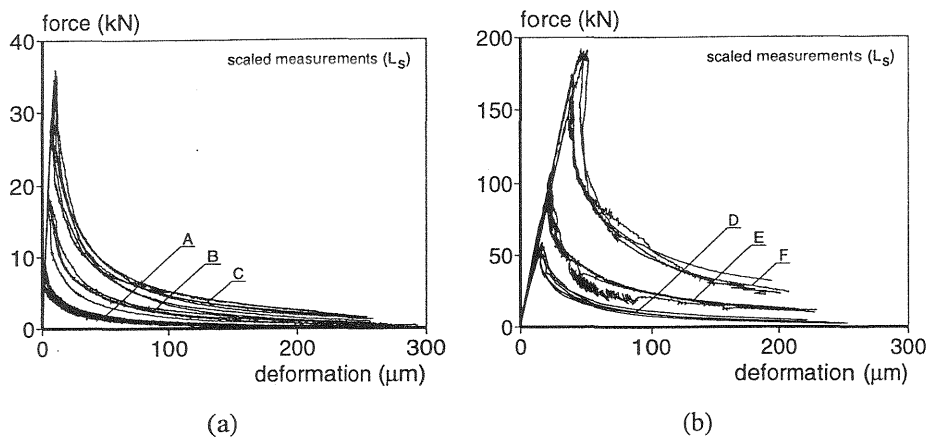


Fig. 3. Overview of force-deformation curves for specimens A, B, C (a) and D, E, F (b)

width of the E and F specimens this meant however that still a considerable residual strength was present at the moment the test had to be stopped.

Fig. 3b clearly shows the effect of using a constant, small control length  $L_c$  (Fig. 2). The softening curves of the F specimens could not have been retrieved if the signal as shown in the graph would have been used to control the test. Because of the large elastic deformations within  $L_s$  the measured deformation decreases at peak load, which would have led to failure of the test if this signal would have been used for feed-back.

By dividing the maximum force recorded during each test by the smallest cross section ( $0.6bD$ ) the nominal stress  $\sigma_N$  was computed. Fig. 4a shows the values of  $\sigma_N$  as a function of the characteristic specimen dimension  $D$  in a log-log plot. To give a more clear picture, individual data for each specimen size have been replaced by mean values and standard deviations

Table 2. Nominal strength

Type (nr)	$\sigma_N$ (MPa)	$c_{A_m} \times \sigma_N$ (MPa)	$c_{f_{c28}} \times \sigma_N$ (MPa)
A (10)	2.54 (0.41)	2.52 (0.41)	2.42 (0.48)
B (4)	2.97 (0.19)	2.89 (0.17)	2.85 (0.25)
C (7)	2.75 (0.21)	2.74 (0.21)	2.59 (0.24)
D (5)	2.30 (0.09)	2.26 (0.08)	2.21 (0.05)
E (4)	2.07 (0.12)	2.01 (0.12)	1.87 (0.12)
F (4)	1.86 (0.16)	1.85 (0.16)	1.85 (0.17)

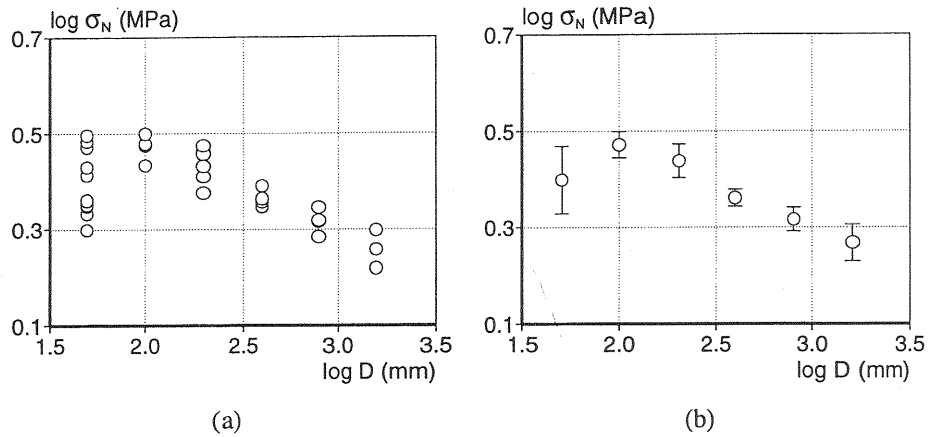


Fig. 4. Individual values (a) and mean values (b) of  $\sigma_N$  vs.  $D$

in Fig. 4b. The corresponding values can be found in Table 2, where the number in brackets in the first column denotes the number of tests.

The followed experimental procedure and the way in which  $\sigma_N$  was computed seem to be quite straightforward. Therefore one could say that a clear indication has been obtained of the size effect on strength for concrete under uniaxial tension. What is not known however, is how sensitive the results are to variations in the testing procedure or the way they were computed. To check these matters two "corrections" have been made to the nominal strength values of Fig. 4a. The first correction concerns the area that was used to compute  $\sigma_N$ . Instead of dividing the ultimate force by  $A (= 0.6bD)$  one could take the projected cross section at the height of crack initiation ( $A_{in}$ ). This area  $A_{in}$  has been determined for each specimen  $i$ , and the origi-

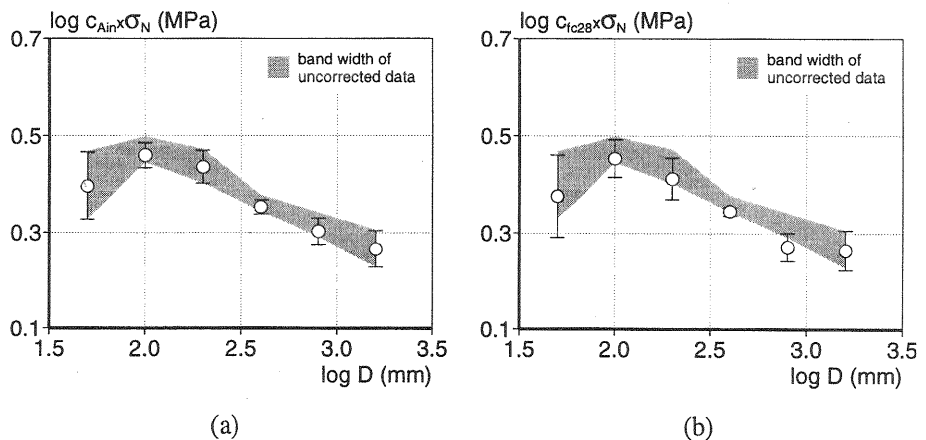


Fig. 5. Influence of correction by  $c_{A_{in}}$  (a) and  $c_{f_{c28}}$  (b) on nominal stress

nal values of  $\sigma_N(i)$  have been multiplied with a correction factor  $c_{A_{in}}(i)$

$$c_{A_{in}}(i) = \frac{A}{A_{in}(i)} = \frac{0.6bD}{A_{in}(i)} \quad (1)$$

The results are shown in Table 2 and in Fig. 5, together with the band width of the uncorrected  $\sigma_N$  values (gray shaded area). A second correction that could be made follows from the fact that the specimens originated from different batches. Suppose the value of the cube compressive strength after 28 days of a certain batch  $j$ ,  $f_{c28}(j)$ , can be regarded as representative for the concrete strength of the uniaxial tension specimens cast from that batch. By multiplying each value of  $\sigma_N(i)$  with a factor  $c_{f_{c28}}(j)$  the influence of the batch strength is compensated. Hence

$$c_{f_{c28}}(j) = \frac{f_{c28}(j)}{f_{c28,max}} \quad \text{with } j = 1, 2, \dots, 10 \quad (2)$$

where  $f_{c28,max}$  is the maximum value of the cube  $D$  compressive strength found among the ten batches. The with  $c_{f_{c28}}$  corrected values of the nominal strength are shown in Fig. 5b and Table 2.

### 3.2 Fracture Energy

Besides the effect of size on the nominal strength also the size dependence of the fracture energy was studied. Following Hillerborg (1985), the fracture energy  $G_F$  is defined as the energy absorbed per unit area in a fictitious crack for complete separation of the crack surfaces. Two values of the fracture energy are considered, namely

$$G_{F_{180}} = \int_0^{180} \frac{F}{A} dw \quad \text{and} \quad G_F = \int_0^{w_1} \frac{F}{A} dw \quad (3)$$

where the value of the projected crack area is taken  $A = 0.6bD$  and  $w_1$  stands for the value of  $w$  at  $\sigma = 0$ . Despite the fact that  $G_{F_{180}}$  is a rather strange parameter when considering the definition of fracture energy, it is merely introduced as a check for the computation of  $G_F$ .  $G_{F_{180}}$  is purely based on measured values, whereas for  $G_F$  the stress-crack opening curves had to be extrapolated. The crack width  $w$  has been computed using the average of the scaled measurements  $L_s$  (Fig. 3). By subtracting the elastic and inelastic pre-peak deformations a crack width of zero is obtained at peak load. The intersection point of the softening curve and the x-axis was computed with the least squares method (Fig. 6a). Although the stress-crack opening curves of specimens A-F are lying in the same region the shape of the curve varies with size (Fig. 6b). With increasing specimen size the peak of the curve decreases whereas the tail rises.

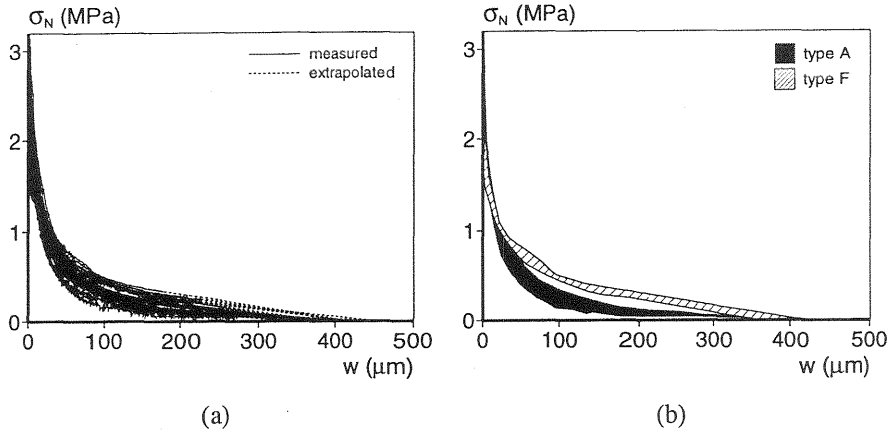


Fig. 6. Overview of stress-crack opening curves for all tests (a) and band width for A and F specimens (b)

The mean values and standard deviations of  $G_{F_{180}}$  and  $G_F$  are plotted in Fig. 7 as a function of  $D$ . The values can be found in Table 3. Note that the trend as found in Figs. 7a and b agrees fairly well. The difference between the  $G_F$  values of the E and F specimens and the small specimens is higher compared to  $G_{F_{180}}$ . This shows the fact that for E and F a relatively large part of the stress-crack opening curve was missing. The general tendency is still the same however: a convergence of the fracture energy to an asymptotic value for large specimen sizes.

Also for the computed  $G_F$  values a sensitivity check was made with regard to the applied surface  $A$ . Here an alternative area  $A_{fi}$  was considered, following from the projection (on the specimen ends) of the intersection

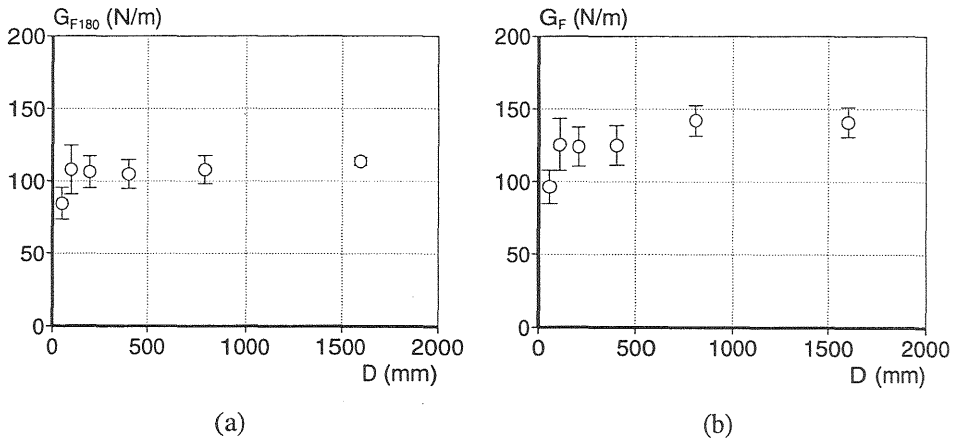


Fig. 7. Fracture energy until  $w = 180\mu\text{m}$  (a) and for total separation (b)

Table 3. Fracture energy

Type (nr)	$G_{F180}$ (N/m)	$G_F$ (N/m)	$c_{A_{fi}} \times G_F$ (N/m)
A (9)	84.49 (11.08)	97.04 (11.83)	96.52 (11.99)
B (4)	108.07 (16.81)	125.67 (17.97)	121.41 (19.08)
C (7)	106.31 (11.00)	124.24 (13.58)	123.48 (13.31)
D (5)	104.89 (10.06)	125.22 (13.70)	122.67 (12.34)
E (4)	107.82 (9.71)	142.31 (10.32)	137.29 (10.60)
F (4)	113.63* (2.78*)	141.12 (10.18)	140.58 (10.48)

\* mean value and standard deviation based on 3 instead of 4 tests

points of the final crack with the edges of the specimen. The correction factor  $c_{A_{fi}}$  for each specimen then reads

$$c_{A_{fi}}(i) = \frac{A}{A_{fi}(i)} = \frac{0.6bD}{A_{fi}(i)} \quad (4)$$

The corrected values for  $G_F$  are presented in Fig. 8 and Table 3.

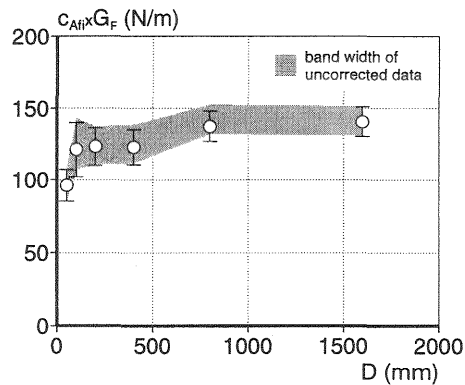


Fig. 8. Influence of correction factor  $c_{A_{fi}}$  on  $G_F$

#### 4 Discussion

The objective of the research on size effect has always been to extrapolate the results found in a certain size range to the asymptotes for extremely small and large sizes. In the uniaxial tension tests on the A specimens the

values for the nominal strength were surprisingly low and showed a considerable scatter (Fig. 4). It is likely that these observations have to be attributed to the small ratio between the width in the center of the specimen and the maximum aggregate size. Consequently most of the cross section, if not the entire cross section, will be subjected to wall effect. This wall effect, in combination with stress concentrations due to large aggregates in the vicinity of the cross section, could be the explanation for the large scatter and the low values for the mean strength of the A specimens. Furthermore, the effect of experimental inaccuracies strongly increases for very small specimen sizes making the results less reliable. Trying to predict strength asymptotes for infinite small specimen sizes therefore seems to be a purely theoretical exercise without any practical use.

With increasing specimen size  $\sigma_N$  was found to decrease, which is consistent with the results of many other researchers. Whether the nominal strength will continue to decrease linearly to zero, as could be concluded from Fig. 4b and the second column of Table 2, is a question that cannot be answered by means of curve fitting. It has been attempted to show that the relation between  $\sigma_N$  and  $D$  is sensitive to possible corrections. Namely when instead of Fig. 4b the curve of Fig. 5b (Table 2 column 4) would be taken, the conclusion would be opposite: for large sizes  $\sigma_N$  reaches a constant non-zero value. The problem of research on size effects lies in the fact that the largest specimens tested are close to the laboratory limits. At the same time they reached only the border of practical structure sizes, which altogether leads to an unrealistic weight of a single set of data. The sensitivity of the mean strength of the F specimens can be illustrated by looking at the values of its constituents. The nominal strengths found for those largest specimens were 1.98 MPa, 1.81 MPa, 1.99 MPa and 1.65 MPa respectively. If the last test had not been conducted the mean value would have been 1.93 MPa instead of 1.86 MPa, which could indicate the bend-over towards a horizontal asymptote instead of a further decrease. The foregoing leads to the conclusion that reducing experimental results to single values can clarify things and be can misleading at the same time, and should therefore be handled with great care.

In the tests it was observed that crack initiation often occurred at the front side of the specimen. Next the crack traversed the specimen to the back side followed by crack growth towards the opposite edge of the specimen. Additional tests showed that the frequent crack initiation at the front side can be attributed to the fact that the specimens were cast horizontally. As a consequence, the casting side of the specimens exhibited a lower strength and stiffness than the mould side, see Van Vliet and Van Mier (1997). This is in accordance with findings of Scheidler (1987) who reported a variation of the concrete stiffness parallel to the direction of casting. Casting effects, or rather the heterogeneous nature of concrete in general, simply exclude uniform deformations during a test. In a uniaxial tension test, which is

carried out in a stiff testing frame while keeping the specimen ends parallel to each other, these non-uniform deformations can be partly counteracted. Also in a set-up with three hydraulic actuators the edges of the controlled specimen region can be kept parallel to each other, Hilsdorf (1963), Ferro (1994). In both cases, however, deformation gradients will still be present within the specimen or the controlled region respectively.

In order to see whether any relation exists between non-uniform deformations and the nominal stress, the *strain* gradients over the specimen thickness (out-of-plane direction) were determined for all specimens. The strain gradients were computed using the deformation difference measured at peak load, between the control LVDT and the LVDT on the same position but on the back side of the specimen. Fig. 9a shows the mean values and the standard deviations of the strain gradients found for the different specimen sizes. The gray shaded area indicates the trend line of  $\sigma_N$  as a function of  $D$ . In Fig. 9b the separate values of the strain gradient are plotted against  $\sigma_N$  and also here the same trend is observed. It is mentioned however that the decrease of the nominal strength with increasing strain gradient does not necessarily hold true for the values of one and the same specimen size. Despite the large scatter, the trend found for the strain gradients at peak load is opposite to that of the nominal stress. This could indicate that with increasing non-uniformity of the deformations of the cross section in general (here over the thickness in particular), locally the ultimate strains are already reached at lower loads. Consequently also  $\sigma_N$  is lower. The increase of the non-uniformity of deformations with specimen size may be due to the increasing system length. When a certain stiffness distribution over the cross section is considered for a small and a long system length, the deformations are larger in the latter case and thus the strains in the outermost fibres. This could be an explanation for the observed size effect on the nominal strength.

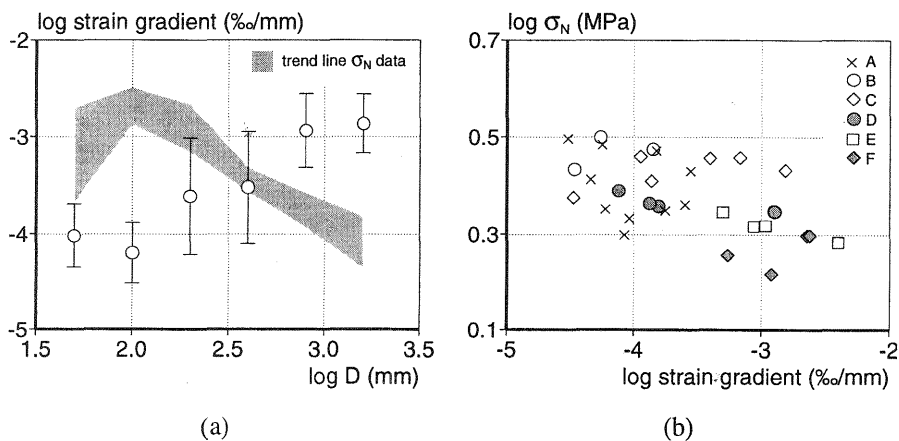


Fig. 9. Mean values of strain gradient (a) and individual values (b)

Also concerning the computed  $G_F$  values a clear trend was found.  $G_F$  increases with specimen size although the tendency seems to be the growth towards a horizontal asymptote for large sizes. This was also observed by among others Wittmann et al. (1990) in tensile splitting tests with ligament lengths up to 600 mm. The considerable contribution of the tail of the stress-crack opening curve for large specimen sizes to  $G_F$  is shown by Figs. 7a and b and Fig. 6b. It seems to be reasonable to extrapolate the tail of the  $\sigma - w$  curve as has been done, although the  $G_F$  values for the large specimen sizes are probably still to low. This is due to the fact that a curved tail of the E and F specimens would have yielded higher values for  $G_F$ . For the A specimens on the other hand, the first part of the stress-crack opening curve has a stronger influence on  $G_F$  than the tail. The low strength values of the A specimens might therefore be the reason for equally low values of  $G_F$ .

An explanation for the variation of  $G_F$  with specimen size can not be given to date. By taking a closer look at the available data and by means of impregnation tests, the authors intend to further study the size effect phenomenon. Additionally, numerical simulations with the lattice model are planned for the next phase of the current size effect study.

## 5 Conclusions

- the nominal strength decreases up to 37% with increasing specimen size which might be due to an increase of strain gradients at peak load
- large scatter and low strength values for the smallest specimens indicate that lower bound strength predictions are not of practical interest
- because of the sensitivity of the nominal strength values extrapolation of the results to large sizes should not be based on curve fitting but on models containing the correct physical mechanisms
- the fracture energy increases with size and tends to become constant for large sizes
- analogous to the strength values also the fracture energy computed for the smallest specimens might have to be regarded with reservation
- the values of the fracture energy are strongly influenced by the tail of the applied stress-crack opening curves

## Acknowledgements

The authors are greatly indebted to Mr. Gerard Timmers for his assistance and enthusiasm in building the experimental set-ups and carrying out the experiments presented in this paper. The work was sponsored through a grant from the Dutch Technology Foundation (STW).

## References

- Bažant, Z.P. (1984). Size effect in blunt fracture: Concrete, rock, metal, **Journal of Engineering Mechanics (ASCE)** **110**(4): 518–535.
- Bažant, Z.P. and Pfeiffer, P.A. (1987). Determination of fracture energy from size effect and brittleness number, **ACI Mat. J.** **6**: 463–480.
- Carpinteri, A., Chiaia, B. and Ferro, G. (1994). Multifractal scaling law for the nominal strength variation of concrete structures, *in* M. Mihashi, H. Okamura and Z.P. Bažant (eds), **Size effect in concrete structures**, E&FN Spon, pp. 173–185.
- Ferro, G. (1994). **Effetti di scala sulla resistenza a trazione dei materiali**, PhD thesis, Politecnico di Torino.
- Hillerborg, A. (1985). The theoretical basis of a method to determine the fracture energy  $G_F$  of concrete, **Mat. & Struct.** **18**(106): 291–296.
- Hillerborg, A., Modéer, M. and Petersson, P.E. (1976). Analysis of crack formation and crack growth in concrete by means of fracture mechanics and finite elements, **Cement and Concrete Research** **6**: 773–782.
- Hilsdorf, H. (1963). Versuchstechnische Probleme beim Studium der Verformungseigenschaften des Betons, **Materialprüfung**, Vol. 5 (11).
- Li, Z., Kulkarni, S.M. and Shah, S.P. (1993). New test method for obtaining softening response of unnotched concrete specimen under uniaxial tension, **Experimental Mechanics** (9): 181–188.
- Mulmule, S.V., Dempsey, J.P. and Adamson, R.M. (1995). Large-scale in-situ ice fracture experiments part II: modeling aspects, *in* J.P. Dempsey and Y.D.S. Rajapakse (eds), **Ice Mechanics**, ASME, pp. 129–146.
- Scheidler, D. (1987). Experimentelle und analytische Untersuchungen zur wirklichkeitsnahen Bestimmung der Bruchschnittgrößen unbewehrter Betonbauteile unter Zugbeanspruchung, **DAfStb**, Vol. 379, pp. 1–94.
- Van Vliet, M.R.A. and Van Mier, J.G.M. (1997). Concrete behaviour under uniaxial tension: Effect of casting and drying conditions, *in* A.M. Brandt, V.C. Li and I.H. Marshall (eds), **Brittle Matrix Composites 5**, Woodhead Publishing Limited, Cambridge, pp. 329–339.
- Van Vliet, M.R.A. and Van Mier, J.G.M. (1998). Experimental and numerical investigation of size scale effects in concrete fracture, *in* R. de Borst and E. van der Giessen (eds), **Material Instabilities in Solids**, John Wiley & Sons Ltd. (in press)
- Walsh, P.F. (1972). Fracture of plain concrete, **Ind. Conc. J.** **46**: 469–470.
- Wittmann, F.H., Mihashi, H. and Nomura, N. (1990). Size effect on fracture energy of concrete, **Eng. Frac. Mech.** **35**(1/2/3): 107–115.